Mobility Modeling in Advanced MOSFETs with Ultra-Thin Silicon Body under Stress

Viktor A. Sverdlov[1], Thomas Windbacher[1], Franz Schanovsky[2], and Siegfried Selberherr[1]

[1]Institute for Microelectronics
[2]Christian Doppler Laboratory for TCAD at the Institute for Microelectronics
TU Wien, Gußhausstraße 27-29/E-360, A-1040 Wien, Austria
e-mail: {Sverdlov|Windbacher|Schanovsky|Selberherr}@iue.tuwien.ac.at

ABSTRACT

We use a two-band **k·p** model to describe the subband structure in strained silicon thin films. The model provides the dependence of the conductivity effective mass on strain and film thickness. The conductivity mass decreases along tensile stress in [110] direction applied to a (001) film. This conductivity mass decrease ensures the mobility enhancement in MOSFETs even with extremely thin silicon films. The two-band **k·p** model also describes the dependence of the non-parabolicity parameter on film thickness and strain. The influence of the subband structure modification on the mobility in advanced MOSFETs with strained ultra-thin silicon body is investigated. It is shown that an increase of subband non-parabolicity in thin films with strain reduces the mobility enhancement due to the conductivity mass modification, especially at higher strain values.

Index Terms: mobility enhancement, strained silicon, stress dependent conductivity mass, non-parabolicity parameter, Monte Carlo simulation.

1. INTRODUCTION

The rapid increase in computational power and speed of integrated circuits is supported by the aggressive size reduction of semiconductor devices. Downscaling of MOSFETs as institutionalized by Moore's law is successfully continuing because of innovative changes in the technological processes and the introduction of new materials. The 32nm MOSFET process technology recently developed by Intel [1] involves new hafnium-based high-k dielectric/metal gates and represents a major change in the technological process since the invention of MOSFETs. Although alternative channel materials with a mobility higher than in Si were already investigated [2, 3], it is believed that strained Si will be the main channel material for MOSFETs beyond the 45nm technology node [3].

With scaling apparently approaching its fundamental limits, the semiconductor industry is facing critical challenges. New engineering solutions and innovative techniques are required to improve CMOS device performance. Strain-induced mobility enhancement is the most attractive solution to increase the device speed and will certainly take a key position among other technological changes for the next technology generations. In addition, new device architectures based on multi-gate structures with better electrostatic channel control and reduced short channel effects will be developed. A multi-gate MOSFET architecture is expected to be introduced for the 22nm technology node. Combined with a high-k dielectric/metal gate technology and strain engineering, a multi-gate MOSFET appears to be the ultimate device for high-speed operation with excellent channel control, reduced leakage currents, and low power budget. Confining carriers within thin Si films reduces the channel dimension in transversal direction, which further improves gate channel control. The quantization energy in ultra-thin Si films may reach a (few) hundred(s) meV. The parabolic band approximation usually employed for subband structure calculations of confined electrons in Si inversion layers becomes insufficient in ultra-thin Si films. A recent study of subband energies and transport in (001) and (110) oriented thin Si films reveals that even the non-parabolic isotropic dispersion is not sufficient to describe experimental data, and a direction-dependent anisotropic non-parabolicity must be introduced [4].

A comprehensive analysis of transport in multi-gate MOSFETs under general stress conditions is

required for understanding the enhancement of device performance. Besides the biaxial stress obtained by epitaxially growing silicon on a SiGe substrate, modern techniques allow the generation of large uniaxial stress along the [110] channel. Stress in this direction induces significant shear lattice distortion. The influence of the shear distortion on subband structure and low-field mobility has not yet been carefully analyzed.

The two-band **k·p** model [5-8] provides a general approach to compute the subband structure, in particular the dependence of the electron effective masses on shear strain. In case of a square potential well with infinite walls, which is a good approximation for the confining potential in ultra-thin Si films, the subband structure can be obtained analytically [9]. This allows an analysis of subband energies, effective masses, non-parabolicity and the low-field mobility on film thickness for arbitrary stress conditions.

In the following we briefly review the main ideas behind the two-band **k·p** model for a valley in the conduction band of Si. Then we shortly analyze the unprimed subband structure in (001) ultra-thin Si films, obtaining analytical dependences for the effective masses and non-parabolicity parameter. With these parameters the non-parabolic subband approximation for the subband dispersions is constructed. The non-parabolic subband dispersions is embedded into the subband Monte Carlo code in order to enable the computation of the low-filed mobility. Results of the mobility enhancement calculations are finally analyzed.

2.CONDUCTION BAND IN SILICON

The subband structure in a confined system must be based on accurate bulk bands of Si including strain. Several options are available. The conduction band dispersions computed with several methods in [100] and [110] directions are compared in Fig.1. The method based on non-local empirical pseudopotentials from [10] is the most accurate as compared to DFT band structure results obtained with VASP [11]. The $sp^3d^5s^*$ tight-binding model with parameters from [12] does not reproduce the anisotropy of the conduction band correctly. In addition, an accurate calibration of the parameters of the $sp^3d^5s^*$ model to describe the modification of the conduction band in strained Si is still lacking.

The **k·p** theory is a well established method to describe the band structure analytically. As illustrated in Fig.1, the **k·p** method reproduces the band structure accurately at energies below 0.5eV, which is enough to describe the subband structure and transport properties of advanced MOSFETs. From symmetry consideration the two-band **k·p** Hamiltonian of a [001] valley in the vicinity of the *X* point of the Brillouin zone in Si must be in the form [6]:

$$H = \left(\frac{\hbar^2 k_z^2}{2m_l} + \frac{\hbar^2(k_x^2+k_y^2)}{2m_t}\right) I + \left(D\varepsilon_{xy} - \frac{\hbar^2 k_x k_y}{M}\right)\sigma_z + \frac{\hbar^2 k_z k_0}{m_l}\sigma_y \quad (1)$$

where $\sigma_{y,z}$ are the Pauli matrices, I is the 2x2 unity matrix, m_t and m_l are the transversal and the longitudinal effective masses, $k_0 = 0.15 \times 2\pi/a$ is the position of the valley minimum relative to the X point in unstrained Si, ε_{xy} denotes the shear strain component, $M^{-1} \approx m^{-1} - m_0^{-1}$, and D=14eV is the shear strain deformation potential [5-8]. The two-band Hamiltonian results in the following dispersions [6]:

$$E = \frac{\hbar^2 k_z^2}{2m_l} + \frac{\hbar^2(k_x^2+k_y^2)}{2m_t} \pm \sqrt{\left(\frac{\hbar^2 k_z k_0}{m_l}\right)^2 + \delta^2} \quad (2)$$

where the negative sign corresponds to the lowest conduction band,

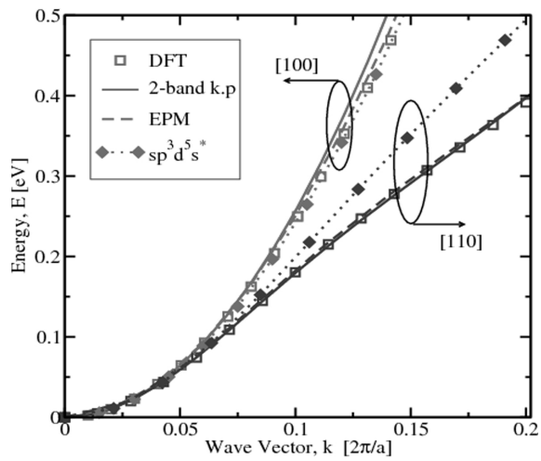

Figure 1. Comparison of bulk dispersion relations close at the minimum of the [001] valleys of the conduction band in [100] and [110] directions. DFT [11] and EPM [7,10] results are similar while the $sp^3d^5s^*$ tight-binding model [12] underestimates anisotropy significantly.

$$\delta^2 = \left(D\varepsilon_{xy} - \hbar^2 k_x k_y / M\right)^2 \quad (3)$$

All moments as well as energies in (2) are counted from the *X*-point of the Brillouin zone. The classical parabolic approximation is obtained from (2), when coupling between the two conduction bands described by the parameter is neglected. Coupling between the bands is small, when the wave vectors $|k_x|, |k_y| << k_0 (M/m_l)^{1/2}$ and shear strain $\varepsilon_{xy} = 0$. Due to band coupling the dispersion (2) becomes non-parabolic in strained Si, if the shear strain component is non-zero, and/or at higher energies.

In order to check the accuracy of (2) we have carried out numerical band structure calculations with the empirical pseudo-potential method (EPM) with parameters from [7,10]. Excellent agreement between the two-band **k·p** model (1) and the EPM results was

found up to energy 0.5eV. The relation (2) is valid in a larger range of energies compared to parabolic dispersion with isotropic non-parabolic correction and can be used to determine the subband structure in thin Si films.

3. SUBBAND EFFECTIVE MASSES

The subband energies can be found analytically for an infinite square well potential which is a good aproximation for an ultra-thin Si film. The dispersion of the unprimed subbands in a [001] thin Si film of thickness t is [9]:

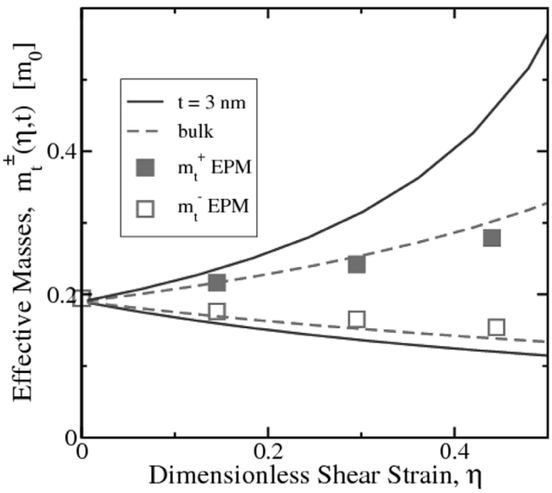

Figure 2. Strain-modified subband effective mass (solid lines). Strain dependence of the transversal mass in bulk silicon is shown by dashed lines and symbols (results of pseudo-potential calculations).

$$E_n(k_x,k_y) = E_n^0(k_x,k_y) - \delta^2 m_1/[2\hbar^2 k_0^2(1-q_n^2)] \qquad (4)$$

where $q_n = (\pi n)/(tk_0)$ and is the subband dispersion for parabolic bands:

$$E_n^0(k_x,k_y) = \frac{\hbar^2\pi^2 n^2}{2m_l t^2} + \frac{\hbar^2(k_x^2+k_y^2)}{2m_t} - \frac{\hbar^2 k_0^2}{2m_l}$$

(4) is valid when

$$\left(1-q_n^2\right)^2 > \delta^2 m_l^2/\hbar^4 k_0^4 \qquad (5)$$

Dispersion (4) describes the subband quantization energy correction due to strain with respect to the valley minimum:

$$\Delta E_n(\varepsilon_{xy}) = -\frac{\pi^2 n^2}{2m_l t^2}\frac{(D\varepsilon_{xy}m_l)^2}{\hbar^2 k_0^4(1-q_n^2)} = \Delta E(\varepsilon_{xy})\frac{q_n^2}{(1-q_n^2)} \qquad (6)$$

(6) is obtained after taking into account the strain-induced valley minimum energy shift $\Delta E(\varepsilon_{xy}) = -(D\varepsilon_{xy})^2 m_l/(2\hbar^2 k_0^2)$ and the dependence of the longitudinal mass m_l on strain [7, 8]:

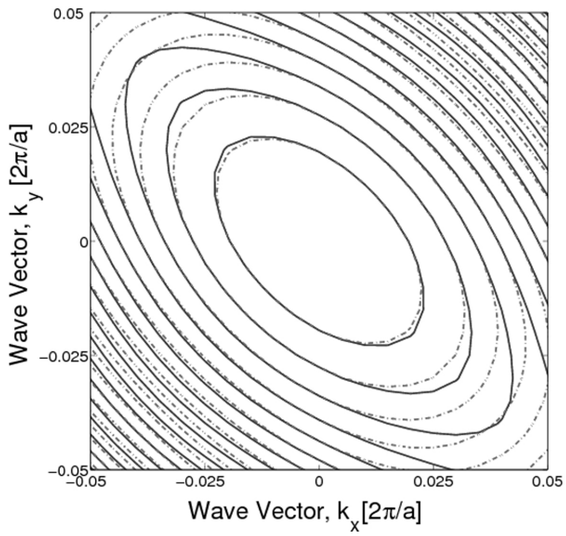

Figure 3. Subband dispersion (4) (solid) as compared to the parabolic approximation (dotted), for a strained film (ε_{xy} = 1%) of thickness t=5.4nm. Spacing between lines is 10meV.

$$m_l(\varepsilon_{xy}) = \frac{m_l}{1-(D\varepsilon_{xy}m_l)^2/\hbar^4 k_0^4} = \frac{m_l}{1-\Delta E(\varepsilon_{xy})/(\hbar^2 k_0^2/2m_l)}$$

(4) also describes corrections to the transversal mass m_t due to strain ε_{xy}, to thickness t, and subband number n:

$$m_t^{\mp} = m_t\left(1 \pm \frac{D\varepsilon_{xy}m_l}{\hbar^2 k_0^2}\frac{m_t}{M}\frac{1}{|1-q_n^2|}\right)^{-1} \qquad (7)$$

Here m_t^- is the effective mass along the direction [110] of tensile stress. In thin films the effective mass depends not only on strain but also on film thickness. (7) is compared to the corresponding dependence in bulk silicon in Fig.2. The thickness dependence of the last term in (7) leads to a more pronounced anisotropy in the transversal mass than in a bulk semiconductor.

A comparison of the dispersion relation (4) to the para bolic approximation with transversal masses (7) for a strained film (ε_{xy} = 1%) of thickness t=5.4nm is shown in Fig.3. Deviations from the parabolic approximation become large for electron energies above 20meV. Therefore, to compute the carrier concentration and mobility in thin Si films the dispersion relation (4) should be used instead of a parabolic approximation at higher carrier concentrations.

4. THE SUBBAND NON-PARABOLICITY

Taking into account the energy shift (6) and the subband effective mass modifications (7) the subband dispersion (4) close to the minimum is written as:

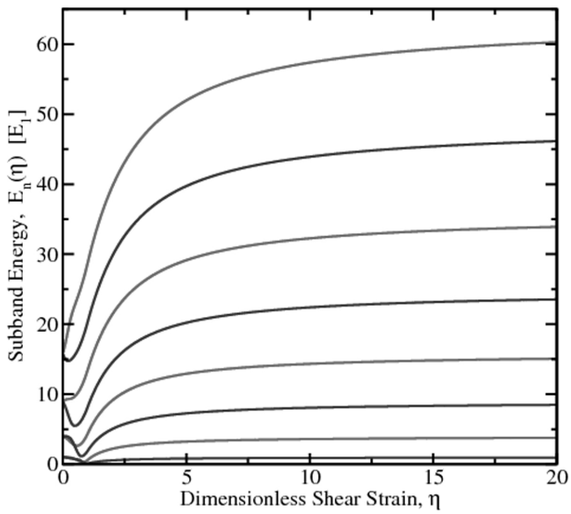

Figure 4. Subband quantization energies E_n from (2) (normalized to the ground subband energy) for a film thickness of 6.5nm. The valley splitting appears for non-zero shear strain η.

$$E_n(k_x,k_y)=\left(\frac{\hbar^2\pi^2n^2}{2m_l(\eta)t^2}-\frac{\hbar^2k_0^2}{2m_l}-\Delta E(\eta)-\Delta E_n(\eta)\right)+\frac{\hbar^2k_-^{-2}}{2m_t^-(\eta)}+\frac{\hbar^2k_+^2}{2m_t^+(\eta)}-\frac{\hbar^2(k_-^2-k_+^2)^2m_l}{8M^2k_0^2(1-q_n^2)}, \quad (8)$$

$\eta = D m_1 \varepsilon_{xy} /(\hbar k_0)^2$

where $k_\pm = (k_x \pm k_y)/\sqrt{2}$ and $\eta = Dm_l\,\varepsilon_{xy}/(\hbar k_0)^2$. The last term in (8) is proportional to the fourth power of the momentum and describes the subband non-parabolicity. We evaluate the dependence of the non-parabolicity parameter $\alpha(\eta,t)$ on strain η and film thickness t by equating the density-of-states obtained from (8) and from the phenomenological expression

$$\frac{\hbar^2k_-^{-2}}{2m_t^-(\eta)}+\frac{\hbar^2k_+^2}{2m_t^+(\eta)}=E\big(1+\alpha(\eta,t)E\big) \quad (9)$$

In the bulk semiconductor a similar procedure [11] yields $\alpha_0 \approx 0.6$ e V^{-1} close to the phenomenological value $\alpha_0 = 0.5$ eV^{-1} routinely used in calculations.

The expression for the density-of-states can be written in the form [12]

$$D(E)=\int\frac{dk_xdk_y}{(2\pi)^2}\delta(E-E_n(k_x,k_y))=\frac{\sqrt{m_-(\eta)m_+(\eta)}}{(2\pi)^2}\int_{E=const}d\varphi\,\frac{1}{2}\frac{\partial\zeta^2(E,\varphi)}{\partial E} \quad (10)$$

where $\zeta^2(E,\varphi)=k_-^2/m_t^-(\eta)+k_+^2/m_t^+(\eta)$ is determined by the expression:

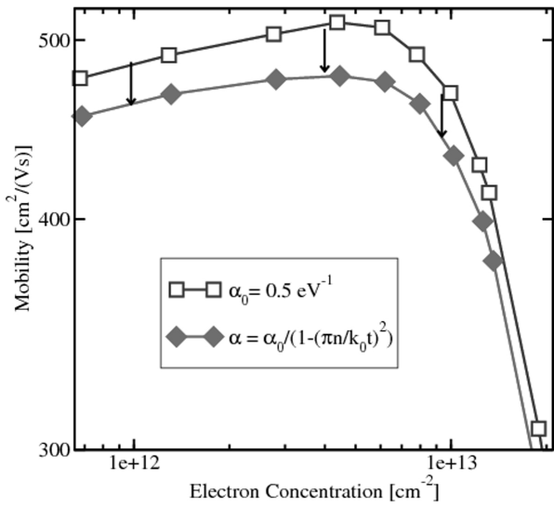

Figure 5. Mobility in a MOSFET with 3nm unstrained UTB film. Due to thickness-dependent subband non-parabolicity the mobility is slightly decreased.

$$E=\frac{\zeta^2}{2}-\frac{\hbar^2m_l}{4M^2k_0^2(1-q_n^2)}\left(m_-\cos^2\varphi-m_+\sin^2\varphi\right)^2\zeta^4 \quad (11)$$

Substituting (11) into (10) and assuming the energy E is close to the valley minimum so that $\alpha E \ll 1$, we obtain the following expression for the non-parabolicity parameter ratio:

$$\alpha(\eta,t)=\alpha_0\frac{1}{1-q_n^2}\frac{1+2\left(\frac{m_t}{M}\frac{1}{1-q_n^2}\eta\right)^2}{1-\left(\frac{m_t}{M}\frac{1}{1-q_n^2}\eta\right)^2} \quad (12)$$

The non-parabolicity parameter depends on the film thickness t via q_n and strain η. We use (7) and (12) in order to evaluate the low-field mobility in FETs with ultra-thin Si films.

5. STRAIN INDUCED VALLEY SPLITTING

A weak coupling between the two valleys located at $k_z = \pm 0.15\,2\pi/a$ around the X-point leading to a so-called valley splitting [15] was neglected while obtaining the subband dispersion relations (4). The valley splitting or, more precisely, the splitting between the two ladders of unprimed subbands reaches several meVs in strongly confined electron systems of Si point contacts [16]. We investigate for the first time how shear strain of arbitrary strength affects the valley splitting.

For each energy E there are four solutions of (2) for the wave vectors k_i (i=1,..,4). The wave function is then a superposition of the solutions with the four eigenvectors. In the two-bands model the wave

$\Delta E_n = 2\left(\frac{\pi n}{k_n t}\right)$

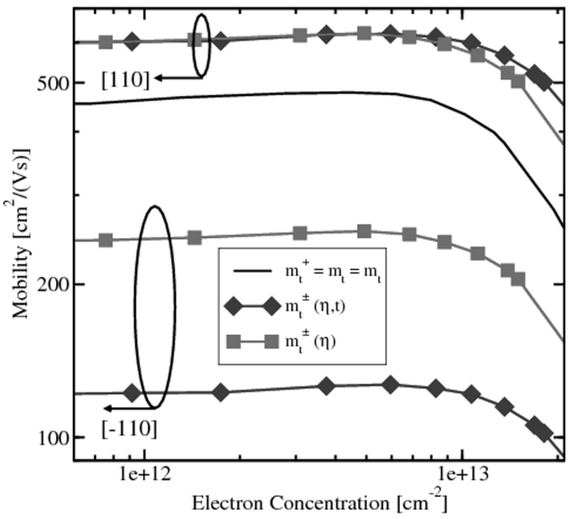

Figure 6. Mobility in a 3nm unstrained (solid line) and with 0.5% strain (diamonds) UTB FET. Squares are obtained with bulk masses and non-parabolicity.

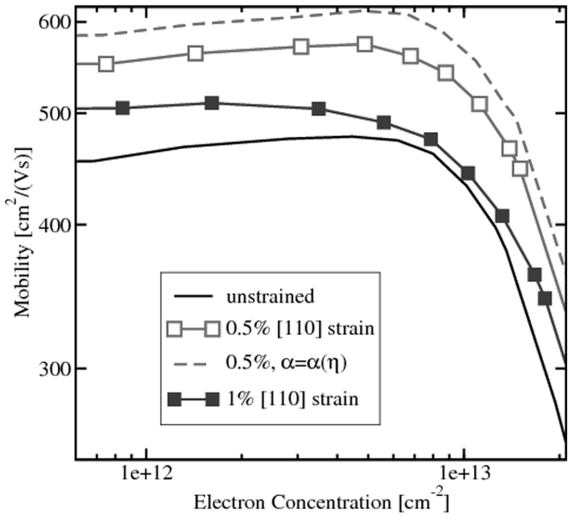

Figure 7. Influence of strain-dependent non-parabolicity on mobility: dashed line denotes strain-independent non-parabolicity, open and filled symbols are for 0.5% and 1% strain, respectively.

function is a spinor with two components. The subband quantization energies are obtained by equating *both* components of the spinor at both interfaces to zero. It results in a system of four linear homogeneous equations for the coefficients in the linear combination. Non-zero solutions exist, when the following equations are satisfied:

$$\tan\left(k_1\frac{t}{2}\right)=\frac{k_2}{\sqrt{k_2^2+\eta^2}\pm\eta}\frac{\sqrt{k_1^2+\eta^2}\pm\eta}{k_1}\tan\left(k_2\frac{t}{2}\right) \qquad (13)$$

Interestingly, the equations (13) coincide with the ones obtained from an auxiliary tight-binding consideration [17]. The ratio in the right hand side depends on the energy E, wave vector k_1, and strain $\eta = m_l D\varepsilon_{xy}/(\hbar k_0)^2$. For zero stress the ratio is equal to one, and the standard quantization condition $(k_1 - k_2)t/2 = \pi n$ is recovered. This condition is obtained from either of the two equations, therefore, the subbands are two-fold degenerate. Shear strain opens the gap between the two conduction bands at the X-point making dispersions non-parabolic. Shear strain renders the equations (13) non-equivalent by removing the subband degeneracy and introducing a valley splitting. The valley split is linear in strain for small shear strain values and depends strongly on the film thickness [7]:

$$\Delta E_n = 2\left(\frac{\pi n}{k_0 t}\right)^2 \frac{D\varepsilon_{xy}}{k_0 t\,|1-(\pi n/k_0 t)^2|}\sin(k_o t) \qquad (14)$$

For higher strain values (14) must be solved numerically. Results of the numerical solutions of (13) for valley splitting are shown in Fig.4. For high strain values the dispersion of the lowest conduction bands becomes parabolic again. The quantization levels in a square well potential are therefore recovered in this limit.

6. SIMULATION METHOD AND RESULTS

A multi-subband Monte Carlo method designed for small signal analysis [18] was used to evaluate the mobility in MOSFETs with a thin Si film. The method is based on the solution of the linearized multi-subband Boltzmann equation and is exact in the limit of vanishing driving fields. A particular advantage of the method is that it includes degeneracy effects due to the Pauli exclusion principle. Degeneracy effects are important for mobility calculations in ultra-thin films, especially at high carrier concentrations.

The multi-subband method requires the subband wave functions and subband energies. They are calculated by solving the Schrödinger and the Poisson equations self-consistently, for each value of the gate voltage. The wave functions are then used to evaluate scattering rates. We include electron scattering with phonons and due to surface roughness. The surface roughness at the two thin film interfaces is assumed to be equal and uncorrelated. We calibrate the parameters of the Gaussian surface roughness correlation function by reproducing the universal mobility curve of Takagi [19] in the inversion layer. The same parameters are then used for mobility calculations in thin film MOSFETs.

An increase of $\alpha_n(\eta)$ leads to an increase of scattering, which results in a slight mobility decrease in a thin film even without stress as shown in Fig.5. Shear strain induces profound modifications in the subband dispersion. First, the dispersion becomes anisotropic, and the transversal mass develops two branches m_t^+ and m_t^-, shown in Fig.2. Due to the thickness-dependent factor $(1-q_n^2)^{-1}$ in (7), the strain-induced subband mass anisotropy is larger than in the bulk. Surprisingly, an even smaller subband transport mass in the tensile

$$\Delta E_n = 2\left(\frac{\pi n}{k_0 t}\right)^2 \frac{D\varepsilon_{xy}}{k_0 t\,|1-(\pi n/k_0 t)^2|}\sin(k_o t)$$

stress direction does not result in a higher mobility enhancement as shown in Fig.6. The reason is the increase (12) of the subband non-parabolicity parameter with strain. This results in a higher density of states and increased scattering with a stronger influence than the transport mass reduction at higher strain, which leads to the mobility enhancement decrease (Fig.7).

7. CONCLUSION

Mobility enhancement in strained MOSFETs with ultra-thin silicon films is investigated. The subband Monte Carlo method which includes the carriers degeneracy is employed to solve the transport Boltzmann equation. In transport calculations, the subband effective masses and the subband non-parabolicity parameter obtained from a two-band **k·p** model are used. The model describes the dependence of the conductivity effective mass on strain and film thickness. A decrease of the conductivity mass along tensile stress in [110] direction of (001) thin silicon film ensures the mobility enhancement in MOSFETs even in extremely thin silicon films. The two-band **k·p** model also describes the non-parabolicity parameter dependence on film thickness and on strain. Inclusion of an increase of the non-parablicity parameter with decreasing film thickness results in a slight decrease of mobility in unstrained films. Dependence of the non-parabolicity parameter on strain also reduces the mobility enhancement due to the strain-induced conductivity mass decrease and may even overpower the enhancement at higher strain values.

ACKNOWLEDGEMENTS

This work was supported in part by the Austrian Science Fund FWF, project P19997-N14, and by funds from FWF, project I79-N16, CNR, EPSRC and the EC Sixth Framework Programme, under Contract N. ERAS-CT-2003-980409 as part of the European Science Foundation EUROCORES Programme FoNE.

REFERENCES

[1] S.Natarajan, M.Armstrong, H.Bost, et al., A 32nm logic technology featuring 2nd-generation high-k + metal-gate transistors, enhanced channel strain and 0.171μm^2 SRAM cell size in a 291Mb array, *IEDM* 2008, pp.941-943.

[2] M.K.Hudati, G. Dewey, S. Datta, et al., Heterogeneous Integration of Enhancement Mode In0.7Ga0.3As Quantum Well Transistor on Silicon Substrate using Thin (<2 um) Composite Buffer Architecture for High-Speed and Low-Voltage (0.5V) Logic Applications, *IEDM* 2007, pp.625-628.

[3] R. Chau, Challenges and Opportunities of Emerging Nanotechnology for Future VLSI Nanoelectronics, *ISDRS* 2007, p.3.

[4] K. Uchida, A. Kinoshita, and M. Saitoh, Carrier Transport in (110) nMOSFETs: Subband Structures, Non-Parabolicity, Mobility Characteristics, and Uniaxial Stress Engineering, *IEDM* 2006, pp.1019-1021.

[5] J.C. Hensel, H. Hasegawa, and M. Nakayama, Cyclotron Resonance in Uniaxially Stressed Silicon. II. Nature of the Covalent Bond, *Phys.Rev.* **138**, A225-A238 (1965).

[6] G.L.Bir and G.E. Pikus, *Symmetry and Strain-Induced Effects in Semiconductors*, J.Willey & Sons, NY, 1974.

[7] E. Ungersboeck, S. Dhar, G. Karlowatz, et al., The Effect of General Strain on the Band Structure and Electron Mobility of Silicon, *IEEE Transactions on Electron Devices* **54**, 2183-2190, (2007).

[8] V. Sverdlov, E. Ungersboeck, H. Kosina, S. Selberherr, Effects of Shear Strain on the Conduction Band in Silicon: An Efficient Two-Band **k.p** Theory, *ESSDERC* 2007, pp.386-389.

[9] V. Sverdlov, G. Karlowatz, S. Dhar, et al., Two-Band k·p Model for the Conduction Band in Silicon: Impact of Strain and Confinement on Band Structure and Mobility, *Solid-State Electronics* **52**, 1563-1568 (2008).

[10] M. Rieger and P. Vogl, Electronic-Band Parameters in Strained $Si_{1-x}Ge_x$ Alloys on $Si_{1-y}Ge_y$ Substrates, Phys.Rev. B 48, 14275-14287, (1993).

[11] The calculations have been performed using the ab-initio total-energy and molecular-dynamics program VASP (Vienna Ab-initio Simulation Program) developed at the Institute for Material Physics of the University of Vienna; G.Kresse and J. Hafner, *Phys.Rev.* B **47**, 558 (1993); ibid. B **49**, 14251 (1994); G.Kresse and J. Furthmueller, *Phys.Rev*. B **54**, 11169 (1996); *Computs.Mat.Sci.* **6**, 15 (1996).

[12] T.B. Boykin, G. Klimeck, and F. Oyafuso, Valence Band Effective-Mass Expressions in the $sp^3d^5s^*$ Empirical Tight-Binding Model Applied to a Si and Ge Parametrization, *Phys.Rev.*B **69**, 115201-1—10 (2004).

[13] C. Jacoboni and L. Reggiani, The Monte Carlo Method for the Solution of Charge Transport in Semiconductors with Applications to Covalent Materials, *Rev.Mod.Phys.* **55**, 645-705 (1983).

[14] M. V. Fischetti, and S. E. Laux, Band Structure, Deformation Potentials, and Carrier Mobility in Strained Si, Ge, and SiGe Alloys, *Journal of Applied Physics* **80**, 2234-2252 (1996).

[15] T. Ando, A.B. Fowler, and F. Stern, Electronic Properties of Two-Dimensional Systems, *Rev.Mod.Phys.* **54**, 437-672 (1982).

[16] S. Goswami, K.A. Slinker, M. Friesen, et al., Controllable Valley Splitting in Silicon Quantum Devices, *Nature Physics* **3**, 41-45 (2007).

[17] V. Sverdlov and S. Selberherr, Electron Subband Structure and Controlled Valley Splitting in Silicon Thin-Body SOI FETs: Two-Band k.p Theory and Beyond, *Solid-State Electronics* **52**, 1861-1866 (2008).

[18] V. Sverdlov, E. Ungersboeck, H. Kosina, and S. Selberherr, Volume Inversion Mobiliy in SOI MOSFETs for Different Thin Body Orientation, *Solid State Electronics* **51,** 299-305 (2007).

[19] S. -I. Takagi, A. Toriumi, M. Iwase, and H. Tango, On the Universality of Inversion Layer Mobility in Si MOSFETs: Part I - Effects of Substrate Impurity Concentration, *IEEE Transactions on Electron Devices* **41**, 2357-2362 (1994).